Effect of Steam on the Homogeneous Conversion of Tar Contained from the Co-Pyrolysis of Biomass and Plastics

Feng Tang
Zhejiang University State Key Laboratory of Clean Energy Utilization
Yuqi Jin (jinyuqi@zju.edu.cn)
Zhejiang University State Key Laboratory of Clean Energy Utilization
Yong Chi
Zhejiang University State Key Laboratory of Clean Energy Utilization
Zhongxu Zhu
Zhejiang University State Key Laboratory of Clean Energy Utilization
Jie Cai
Zhejiang University State Key Laboratory of Clean Energy Utilization
Zhirui Li
Zhejiang University State Key Laboratory of Clean Energy Utilization
Minjie Li
Zhejiang University State Key Laboratory of Clean Energy Utilization

Research Article

Keywords: Co-pyrolysis tar, Steam, Chain compound, Aromatic hydrocarbon

Posted Date: May 24th, 2021

DOI: https://doi.org/10.21203/rs.3.rs-454069/v1

Version of Record: A version of this preprint was published at Environmental Science and Pollution Research on July 20th, 2021. See the published version at https://doi.org/10.1007/s11356-021-15313-3.

Abstract

The co-pyrolysis tar formed from microcrystalline cellulose (MCC) and polyethylene (PE) was used to study their further conversion path under the effect of steam. This paper addressed the yield and transformation of tar with different steam/feedstock mass ratios (S/F= 0.8, 1.6) in a two-stage fixed-bed when the two stages furnace temperature was set at 600℃ and 800℃, separately. Compared with pyrolysis, steam promoted tar cracking effectively, the tar yield decreased at least 1/3. However, with the addition of steam, the cracking effect of tar is not further improved. The tar yield depended more on the PE content in the mixture, which was enhanced with PE increment. Besides, the H/C atom ratio was related to the conversion path of tar. Steam was beneficial to the cracking of compounds, but the generated hydrogen radicals affected the direction of the subsequent reaction. The steam mainly promotes the cracking of long-chain hydrocarbons, accompanied by cyclization and aromatization when the steam was limited. Nevertheless, these reactions were hindered when the steam was excessive due to the apparent effect of hydrogenation. In this process, the short-chain hydrocarbons come to recombine instead of cyclization and aromatization.

1. Introduction

The environmental treatment and resource utilization technologies of waste are still facing a bottleneck. For example, as the composition and content of waste always fluctuate randomly, these unstable feedstocks are not conducive to the operation of thermal disposal equipment. There have been many studies focused on the interaction of different waste components in the pyrolysis process by the thermal gravimetric analyzer(Sørum et al. 2001; Dong et al. 2007; Tang et al. 2018). Furthermore, Wen (Wen et al. 2004) designed a thermogravimetric system in which more massive typical organic components of MSW (about 10g) were able to be analyzed. They found the waste components such as biomass and textiles are difficult to interact with each other, so the properties of these mixtures could be predicted accurately according to the features of each component during pyrolysis; but if there are polymers (e.g., plastics) in the mixture, the interaction between the components was not able to be ignored. Based on the experimental results mentioned above, they also established a prediction model for MSW pyrolysis by using the principle of chemical reaction kinetics and the theory of B.P. neural networks(Wen et al. 2005). Similarly, Long proposed the pseudo-component method (Long et al. 2017) for predicting the combustible solid waste materials properties.

Researchers have also completed many enlightening studies based on adding catalysts and changing the experient conditions to improve the reaction effectivity. For all of these methods, introducing a gasification agent is also convenient, except for adjusting the temperature. For instance, steam was introduced (Pinto et al. 2002; Wilk and Hofbauer 2013), and the excess air ratio was even varied by adding air or oxygen(Pinto et al. 2012; Wilk and Hofbauer 2013; Giovanna Ruoppolo et al. 2013; Lopez et al. 2015; Pinto et al. 2016). Moreover, there were also reported that adopting the gasification agent with catalyst was able to realize a synergistic effect(Lopez et al. 2015; Zheng et al. 2016). As for the co-pyrolysis/gasification, there are always accompanied by the formation of by-products like tar. Pinto et al. (Pinto et al. 2016) compared the effects of different gasification agents on tar cracking and found that steam promoted the destruction of tar by steam reforming reactions, and air favored the partial oxidation of tar compounds. Nevertheless, they also reported

that the syngas higher heating value (HHV) decreased with the rise of oxygen. Hence, steam is an optimal choice to reduce the tar yield.

To study the role of steam in the mixture co-pyrolysis/gasification process, a continuous and stable operation is indispensable, which is also conducive to prolong equipment life and cut down the potential fluctuations of emissions. **Table 1** summarizes the experimental condition of some typical equipment for the mixture co-pyrolysis/gasification process under the effect of steam. It can be concluded that 800–900 ℃ is the ideal temperature range for steam to play its role. As for the removal mechanism of tar, some previous studies provided different explanations. Lopez et al. (Lopez et al. 2015) reported the H_2 yield was able to reach 60%(V/V), and they thought the co-feeding of high-density polyethylene(HDPE) had generated an interesting synergetic effect involving the reduction of both tar and char yields. This result agrees with Wilk et al. (Wilk and Hofbauer 2013), who believed the tar content in the product gas was considerably lower than that presumed, and less CH_4 and C_2H_4 were formed. Ahmed et al.(Ahmed et al. 2011a) attributed the interaction between biomass and plastics to the PE, which acted as a hydrogen donor for radicals generated from woodchips pyrolysis, resulting in stabilizing those radicals and producing a higher yield of total hydrocarbons than that expected by the weighted average yield. On the other hand, woodchips char might have played a role in absorbing volatiles from PE and promoting steam-hydrocarbons reforming reaction to result in more hydrogen than expected by the weighted average yield alone.

As mentioned above, there has been a clear grasp of the production yield (including syngas, tar, and char) under the steam effect of co-pyrolysis/gasification. However, tar transformation, especially for the high tar yield formed at 600 ℃(Fagbemi 2002; Li et al. 2004), is still worth researching.

This paper focused on the change of tar yield and composition under different amounts of steam. In particular, this experiment was based on the tar produced from the co-pyrolysis of MCC and PE at 600℃, which provided more reliable tar compositions than using a few representatives(Barbarias et al. 2016a). Moreover, the co-pyrolysis tar was further transformed at 800℃, and the effect of steam was analyzed without considering the potential role of char.

Table 1

Comparison between different co-pyrolysis/gasification processes with steam.

Furnace type	Feedstock	Temperature	feed rate	Steam/ Feedstock	Flow rate	Reference
Bubbling fluidized bed	Wood pine and PE	730–900°C	5.7–12.5 g/min	S/F= 0.4–0.9	Steam 5.3g/min	(Pinto et al. 2002)
Dual fluidized-bed	Four types of plastic material of different origins and soft wood pellets	Gasification 850°C Combustion 900°C	-	S/C= 1.8-2.3[a]	(Gasification) Steam 13-18.9kg/h (Combustion) Air 52.7-56.3nm3 /h	(Wilk and Hofbauer 2013)
Conical spouted bed	Pinewood sawdust and HDPE	900°C	1.5g/min	S/F = 1	Water 1.5 ml/min Nitroge 20 l/min Air 20 l/min	(Lopez et al. 2015)
External circulating radial-flow moving bed	Pine sawdust and bituminous coal	Pyrolysis 500–700°C Gasification 750–850°C Combustion 850°C	0.2kg/h	S/F= 0.3–1.9	(combustion) Air 4.2–4.6 Nm^3/h	(Tursun et al. 2016)

[a] S/C = Steam/Carbon(g/g)

2. Materials And Methods

2.1. Materials

MCC and PE were chosen to represent biomass and polymer, respectively. The MCC is a crucial component of plant cellulose(Shurong 2017), and the PE accounts for 62.5-74.8% of plastic waste(Areeprasert et al. 2017). The basic properties of feedstock were analyzed by 5E Series-MAG6700 Proximate Analyzer and 5E Series-CHN2000 Ultimate Analyzer separately.

2.2. Thermogravimetric analysis

The thermal characteristics of MCC and PE were studied by thermogravimetric analysis (NETZSCH, TGA5500, Germany). Approximately 10 mg of samples were used in the programming-temperature TGA pyrolysis process with a heating rate of 10 °C/min from ambient temperature to 1000 °C under 70 mL/min high-purity nitrogen. Before the experiment started, several blank experiments were carried out under the same conditions. And then, the blank TGA curve was used for baseline corrections.

2.3. Fast pyrolysis analysis

Fast pyrolysis experiments were performed in a single shot micropyrolyzer (PY-3030D, Frontier Laboratories, Japan) and the products were analyzed in a gas chromatograph that was equipped with a mass spectrometer (GC/MS, QP2010, Shimadzu, Japan). About 2 mg samples were rapidly heated to a preset temperature (600℃) and hold for 12s. Experiments were performed in a helium (He, 99.99 % purity) environment. The volatiles emitted via this fast heating were carried by He to the GC/MS and separated by an Rtx-5ms(DB-5\HP-5) capillary column (30 m×0.25 mm×0.25 μm). The carrier gas (He) flow was 1 ml/min, and the split ratio was 30:1. The oven temperature was initially kept at 50℃ for 1 min. Then, continuously heated to 300℃ at 15 ℃/min, and maintained at 300 °C for 20 min. The heated transporting tube and injector temperature were set at 300 C. The chromatographic peaks were identified with the help of NIST mass spectral data library.

2.4 Experimental equipment and conditions

A scheme of the bench-scale plant used for mixture wastes (consisting of MCC and PE) treatment is shown in **Fig 1**. The apparatus mainly consists of a reverse L tubular reactor made of steel (outer diameter: 40 mm, inner diameter: 30 mm). The tubular reactor consisted of two stages made of steel (outer diameter: 40 mm, inner diameter: 30 mm), with each length of 500mm. The feedstock was delivered into the pyrolysis reactor through a screw feeder installed in the tubular channel. After the feedstock was pyrolyzed about 25 minutes in the first stage, the remaining residue was sent into the slag hole when the separated gaseous products (including syngas and tar) went through the second stage to react with saturated steam under the suction of the vacuum pump at the end. Then, all the products passed through the condenser and tar trap in sequence to separate the steam and tar. The remaining non-condensate gases were also disposed of safely by other means. After continuous operation for 60 min, the feed was stopped, and the steam flow was maintained for another 20 min. Each experiment was repeated at least three times to ensure the reproducibility of the results. The experimental conditions are listed in **Table 2**.

Table 2

Operation parameters of the experiments.

NO.	1	2	3	4	5	6
MCC to PE ratio (g/g)	4:1	4:1	2:1	2:1	1:0	0:1
Steam to feedstock ratio (g/g)	0.8	1.6	0.8	1.6	0	0
Nitrogen flow rate（L/min）	1.7	0.4	1.7	0.4	3.0	3.0
Total feedstock（g）	80					
Fuel feeding rate（g/min）	1.33					
First stage temperature (°C)	600℃					
Second stage temperature (°C)	800℃					
Connecting section temperature (°C)	180℃					

2.5 Tar pretreatment and analysis

Before the tar analysis, there were a series of pretreatments: 1) transferred the mixture solution collected from the tar trap and washed it with 50 ml dichloromethane each time, repeating three times; 2) separated moisture and organic solvents from the collected solutions, including the washing solution, by a separation funnel; 3) added anhydrous sodium sulfate to the organic solution to further remove the moisture; 4)separated the tar from the filtered organic solvent (a mixture of tar and dichloromethane) by rotating evaporators following the European standard (CEN/TS15439: 2006). Dichloromethane is an efficient solvent that can absorb the heavy components of tar well. Many studied used it to wash and collect tar formed from the thermal treatment of solid waste(Hu et al. 2017; Lu et al. 2018, 2019).

The composition of tar was measured by a GC-MS analyzer (7890B-5977A, Agilent Technologies, Germany). The injector and the transfer line were set at 270 and 250 °C, respectively. After 5 min at 50 °C, the oven raised to 270 °C at a rate of 15 °C/min and then maintained at 270 °C for 10 min. In the mass spectrometer, electron ionization (E.I.) energy was used for ionization. The ion source temperature was maintained at 200 °C. The volume of each injection was 0.2 μL, and the split ratio was 10:1. Identification of compounds was performed according to library data. There were three parallel samples of each experiment condition measured by GC-MS, and the average results are shown in **Table S2** and **Table S3**.

3. Results And Discussion

3.1 Material characteristic

The proximate and ultimate analysis of materials is listed in **Table 3**. The two materials exhibit entirely different characteristics: compared to the MCC, there is a small content of moisture and fixed carbon in PE, while elements content such as carbon and hydrogen are higher. Besides, the low oxygen content is also a typical characteristic of PE.

Thermogravimetric (TG) and differential thermogravimetric (DTG) curves of MCC and PE were given in Fig. 2. The release of moisture from MCC occurs a small amount of weight loss until 150°C, and the structural breakdown starts nearly at 287°C and ends at about 397°C with a maximum rate at 358°C. In this phase, MCC is depolymerized to oligosaccharides and then cracks to volatiles and non-condensable gas. Unlike polyvinyl chloride (PVC), which has two prominent peaks(Tang et al. 2018), PE has only one weight loss peak. The main decomposition step occurs between366 and 508°C, with the maximum mass loss rate at 471°C. Therefore, the volatiles from PE generally start to evolve at a higher temperature range than those from MCC. It suggests the existence of a combination of interactions between the volatiles released and fixed carbon(Ahmed et al. 2011b).

Table 3

Proximate and ultimate analysis of materials.

Components	Proximate analysis(%)				Ultimate analysis(%)					Qb,ad(kJ/kg)
	M_{ad}	A_{ad}	V_{ad}	F.C.$_{ad}$	C_{ad}	H_{ad}	N_{ad}	S_{ad}	O_{ad} [a]	
MCC	5.83	-	88.12	6.05	41.92	4.59	0.08	0.19	47.39	16561
PE	0.08	0.05	99.73	0.14	85.99	11.49	0.24	1.19	0.96	47141
[a] by difference.										

3.2 Fast Pyrolysis Products Analysis

Fast pyrolysis of the MCC and PE produced significantly different primary products. Figure 3 shows the chromatograms of products and marks the main compounds, and the details of detectable and recognizable compounds are listed in**Table S1**. It should be noted that the detectable compound was that whose concentration was above the detection limit, while the identifiable compound was that whose peak area was comparatively large, and were identified by the NIST library in this work. The following discussion on the amount of product components is based on the percent peak area in chromatograms. As seen in Fig. 3, the primary pyrolysis products of the MCC are compounds with oxygenated groups, such as ethanedial, methyl glyoxal, β-D-Glucopyranose, 1,6-anhydro-. These compounds with oxygenated groups are produced from a series of reactions (including cracking, dehydration, depolymerization, etc.) of glucose, because cellulose is a linear macromolecular polysaccharide that consists of a long-chain of glucose units linked by β-1,4-glycosidic bonds(Shurong 2017). As for the PE, the main products obtained during the thermal decomposition are linear hydrocarbons, while a low proportion of aromatics is also present(Wampler 1989; Hájeková and Bajus 2005; Marcilla et al. 2006). In terms of carbon number, these chain hydrocarbons and their derivatives between C_{11} and C_{20} are the most considerable (47.62%). Others, such as more than C_{20} and C_4-C_{10}, account for 35.64% and 16.78%, respectively.

3.3 Effect Of Steam On Tar Components

Figure 4 shows the tar yield of two mixing ratios under different steam contents. As a note, the tar yield at pyrolysis is based on the linear weighting result of single component pyrolysis tar. Compared with pyrolysis, steam promoted tar cracking significantly, and tar yield decreased by at least half at MCC: PE = 4:1. It illustrates that steam plays an essential role in tar cracking. However, the cracking effect of tar is not further improved with the increase of steam. Accordingly, the deciding factor of tar yield is certainly the proportion of PE in the mixture rather than the growing steam amount.

As shown in **Table 4**, the addition of steam affects the element content of tar products. For example, the carbon content increases with steam enhancement, while the oxygen content is contrary. It suggests that steam can stimulate the gasification of tar because the polymerization and the boundary reaction promote carbon deposition formation (Vicente et al. 2014; Montero et al. 2015; Barbarias et al. 2016b), the content of carbon elements in tar products increased. Finally, the compounds react with steam and further crack into non-condensable gas, such as CO and CO_2, thus reducing the content of oxygen in tar.

Consistent with Lu et al. (Lu et al., 2018) results, the H/C ratio of tar also increases with the addition of PE content in the mixture. More importantly, the changing trend of the H / C ratio of tar in the two mixed rates is different. As shown in **Table 4**, when there is a small PE amount in the mixture (MCC: PE = 4:1), the H/C ratio increases with steam addition, but the trend is the opposite at MCC: PE = 2:1. All of these can be attributed to the different transformation paths of tar under the steam effect. It needs to consider the relationship between the PE account in the mixture and the additional steam synthetically. Because when the PE content in the mix is high, the leading role of steam is to promote the cracking of tar, accompanied by cyclization and aromatization. However, if the proportion of PE is not too high, this process can be realized by a small amount of steam. The superfluous steam can promote the recombination of chain hydrocarbons to produce new chain hydrocarbons and its derivatives to make the rising of the H/C ratio. It will be further explained in the next part.

Table 4

Ultimate analysis of tar.

Element	MCC:PE = 4:1		MCC:PE = 2:1		MCC	PE
	S/F = 0.8	S/F = 1.6	S/F = 0.8	S/F = 1.6	S/F = 0	S/F = 0
C	81.50	87.51	80.40	86.73	62.72	83.71
H	5.71	7.51	8.21	7.44	5.34	10.14
N	0.22	0.20	0.23	0.22	0.36	0.43
O[a]	12.57	4.78	11.16	5.61	31.58	5.72
H/C[b]	0.841	1.030	1.225	1.029	1.022	1.45
[a] by difference; [b] atomic ratio.						

The detectable tar products were identified according to chromatographic peaks, and their amount was determined from the peak area in GC–MS chromatograms (shown in Fig. 5). As seen in **Table S3**, there are negligible cross-over products, which agrees with the result of biomass/plastics co-pyrolysis(Bhattacharya et al. 2009; Li et al. 2014). Most of the products are consistent with those previously observed in the pyrolysis of the two individual components. It is worth noting that the proportion of PE in the mixture has a significant effect on the characters of the tar. For instance, when the PE content in the mixture is higher (MCC: PE = 2:1), there are more chain hydrocarbons and their derivatives under the effect of steam. Nevertheless, aromatic compounds are the dominant components in the tar at MCC: PE = 4:1.

The major compositions of tar have been quantified and summarized in **Table 5**. There is an apparent change of o-heterocycles and alicyclic compounds: both of them are inversely proportional to the steam amount under two different mixture ratios. It indicates that the two compounds are effectively cracked or converted into more stable compounds such as aromatic and chain compounds with steam addition. For example, the o-heterocycles can be converted into more stable aromatic compounds by the Diels-Alder reaction(Carpenter et al. 2010; Göransson et al. 2011; Lopez et al. 2015).

Table 5

Detailed distributes of major tar compounds.

Compounds	MCC:PE = 2:1		MCC:PE = 4:1	
	S/F = 0.8	S/F = 1.6	S/F = 0.8	S/F = 1.6
Main types of compounds(% area)				
Chain compounds [a]	68.81	65.87	6.81	41.12
O-heterocycles [b]	0.81	-	4.78	1.43
Alicyclic compounds [c]	6.52	1.69	8.61	3.22
Aromatic compounds	23.86	32.44	79.80	54.23
Aromatic compounds(% area)				
Toluene	1.80	3.70	14.06	6.35
Aromatic acids [d]	-	7.23	11.59	13.29
Xylenes [e]	2.61	4.30	9.60	5.54
Other alkylbenzenes [f]	3.13	1.29	8.06	6.15
Alkenylbenzenes [g]	5.87	9.47	13.91	5.37
Alkynylbenzenes [h]	-	-	3.46	-
Indenes [i]	3.99	2.53	6.46	5.97
Polycyclic aromatic compounds [j]	6.46	3.92	12.66	11.56

[a]Chain compounds (1,5-Hetadien-3-yne; 1,3,5-Heptatriene, (E,E)-; 1-Decene; 1-Undecene; 3-Undecene; 3-Dodecene; 7-Tetradecene; 1-Pentadecene; 1-Heptadecene; 3-Octene,(z)-; 1-Nonene; 1-Tridecene; 3-Tetradecene; 2-Tridecene; Cetene; 1-Octadecene; 1-Eicosene; 17-Pentatriacontene; 1-Tetradecanol; 2-Hexadecanol; n-Nonadecanol-1; Ethanol, 2-(9-octadecenyloxy)-, (E)-; Behenic alcohol; 1-Tricosanol; 1-Tetradecanol; 2-Hexadecanol; 1-Hexadecanol,2-methyl-; n-Nonadecanol-1; 2,4-Decadien-1-ol; 2,6-Octadien-1-ol,2,7-dimethyl-; Hexanoic acid, decyl ester; Oleic Acid; 1-Hexadecanol, acetate; Oleic acid, eicosyl ester; 9-Hexadecenoic acid, eicosyl ester, (Z)-)

[b]O-heterocycles (Furfural; n-Decylsuccinic anhydride; [(+)-Noe's reagent; (+)-MBF-OH dimer)

[c]Alicyclic compounds (1,3,5,7-Cyclooctatetraene; 1,3,5-Cycloheptatriene;Bicyclo[2.1.1] hexan-2-ol,2-ethenyl)

[d] Aromatic acids (o-Tolylacetic acid; 2-Butenoic acid,3-methyl-,2-phenylethyl ester)

[e] Xylenes (o-Xylene; p-Xylene; Benzen,1,3-dimthyl)

[f] Other alkylbenzenes (Ethylbenzene; Benzene,1-ethyl-3-methyl-)

[g] Alkenylbenzenes (Styrene; Benzene,1-ethenyl-4-methyl-; Benzene,1-ethenyl-3-methyl-; Benzene,1-ethenyl-2-methyl)

Compounds	MCC:PE = 2:1		MCC:PE = 4:1	
	S/F = 0.8	S/F = 1.6	S/F = 0.8	S/F = 1.6
[h] Alkynylbenzenes (3-Methylphenylacetylene; 1-Propyne,3-phenyl-)				
[i] Indenes (Indene; 1H-Indene, 1-ethylidene-; 1H-Inden,3-methyl-)				
[j] polycyclic aromatic compounds (Naphthalene; Naphthalene, 1-methyl-; Fluorene)				

The chain compounds are the essential components of tar, and their proportion is significant affected by the different proportions of PE in the mixture. As presented in **Table 5**, when MCC: PE = 2:1, the proportion of open chain compounds decrease with steam enhancement. However, the open-chain compounds are proportional to the amount of steam at MCC: PE = 4:1. Significantly, most of the chain compounds are unsaturated hydrocarbons and their derivatives. The receptors of hydrogen radicals (such as acids and aldehydes) formed from the co-pyrolysis of the mixture are easier to bond with hydrogen(Li et al. 2014). Thus the competition for hydrogen radicals is unfavorable to the conversion of chain hydrocarbons from unsaturated to saturated.

According to the number of carbon atoms, the chain compounds can be divided into three categories, as shown in Fig. 6. These compounds mainly concentrate on C_{10}-C_{20} and are positively correlated with the steam amount, while the compounds whose carbon chain length over 20 are cracked. It can be accounted for that long-chain compounds are easily converted into shorter and simpler hydrocarbons with steam promotion (Rama et al. 2014). Furthermore, when PE accounts for a large proportion in the mix (MCC: PE = 2:1), the steam mainly promotes the cracking of long-chain hydrocarbons and their derivatives as much as possible. At the same time, the intermediate products, such as conjugated dienes and substituted olefins, can be further cyclized and aromatized(Lukyanov et al. 1994; Adjaye and Bakhshi 1995; Aguado et al. 2001; Gayubo et al. 2004; Li et al. 2014). Conversely, when there is a small part of PE in the mixture, this process can be achieved at S/F = 0.8. With the continual addition of steam, the cyclization and aromatization process may be inhibited. Even the short-chain hydrocarbons and their derivatives(< C_{10}) may bond with each other under the action of O/H/OH radicals to form new chain hydrocarbons and their derivatives with the carbon chain length between 10 and 20 when the steam is excessive (S/F = 1.6).

On the other hand, the change of aromatic compounds is also proof of the above point. As listed in **Table 5**, aromatic compounds show an opposite trend with the increase of steam under the two mixing ratios of mixtures. When there is a higher PE content in the mixture (MCC: PE = 2:1), the aromatic compounds are positively correlated with steam, while the ratio of mixture changes to MCC: PE = 4:1, the amounts of aromatic compounds decline apparently. In general, the proportion of total aromatic compounds is greatly affected by the change of monocyclic aromatic hydrocarbons (MAHs). For instance, the total ratio of MAHs increases at MCC: PE = 2:1. In view of the cracking of chain compounds and alicyclic compounds, they provide abundant dienes and dienophiles to cyclization and aromatization with the effect of steam. In addition, the increase of steam also stimulates the formation of aromatic acids (such as o-tolylacetic acid, 2-

butenoic acid, 3-methyl -, 2-phenyl ester), which may reduce the possibility of further cyclization and aromatization of MAHs, which is also the reason for the decrease of indenes and naphthalenes in **Table 5**.

On the contrary, the MAHs (such as alkylbenzenes, alkenylbenzenes, and alkynylbenzenes) greatly decrease, which is an important reason for the apparent decrease of the proportion of total MAHs at the MCC: PE = 4:1. It can be attributed to the fact that long-chain compounds can be effectively cracked with less steam (S/F = 0.8), and the products, such as dienes and dienophiles, can further react with each other to realize cyclization and aromatization. If the steam continues to be added (S/F = 1.6), these dynamic equilibriums may be broken. The hydrogen radicals supplied by the spared steam promote the hydrogenation reaction, which competes with cyclization and aromatization. And there is no affluent diene and dienophile for cyclization and aromatization, making it difficult to keep the generation of MAHs and even polycyclic aromatic hydrocarbons (PAHs) as much as possible. In particular, there is still a slight increase in aromatic acid. Therefore, these different reaction paths eventually reach a new equilibrium: the hydrogenation can effectively avoid further cyclization and aromatization to form PAHs [32], while the limited MAHs are more likely to convert to aromatic acid with the steam effect.

Based on the above analysis, the conversion paths of compounds can be summarized as steam contributes to the cracking of long-chain hydrocarbons and their derivatives, while short-chain hydrocarbons, such as diene and dienophile, can further promote cyclization and aromatization. On the other hand, hydrogen radicals generated from the reaction process can promote hydrogenation, which will inevitably compete with cyclization and aromatization. When the proportion of PE in the mixture is large, steam mainly promotes the cracking of long-chain hydrocarbons, and the abundant products such as unsaturated short-chain hydrocarbons are conducive to further cyclization and aromatization. In this situation, although hydrogen radicals can promote hydrogenation that is not conducive to the further reaction of MAHs to PAHs, there is a small influence on product distribution. When there is less PE in the mixture, the above reactions can be realized by introducing less steam. However, if the addition of steam is excess, more hydrogen radicals will participate in the hydrogenation, which is obviously not conducive to the formation of aromatic compounds. Meanwhile, the recombination between short-chain hydrocarbons will be strengthened.

4. Conclusions

In this paper, the tar formed from the MCC and PE co-pyrolysis further transformed with the steam addition in a two-stage fixed-bed were studied. It addressed the conversion of tar yield and composition under different amounts of steam.

Compared with pyrolysis, steam makes for the cracking of tar. In terms of the tar yield, it cut down at least one-third. In addition, compared with the further change of steam amount, the influence of the PE content in the mixture is more significant. The tar yield is about twice as before when the MCC: PE varies from 4 to 2.

As for the tar properties, the carbon content increases with steam addition, while the oxygen content decreases. Moreover, the changing of H/C is related to the conversion path of tar. Steam promotes the cracking of compounds to produce hydrogen radicals. And further reactions, including cyclization, aromatization and hydrogenation, need the participation of hydrogen radicals. Thus, when the steam

content is limited, it mainly stimulates the cracking of long-chain compounds. On the contrary, excessive steam facilitates the recombination of short-chain hydrocarbons, and the effect of hydrogenation can not be ignored, which is not conducive to cyclization and aromatization.

5. Declarations

Acknowledgments

This work was supported by the National Key R&D Program of China [Grant NO. 2018YFD1100602].

Authors contribution Feng Tang completed the experiment and wrote the original draft. Yuqi Jin and Yong Chi proposed this study and reviewed the manuscript. Zhongxu Zhu helped revised the manuscript and put forward constructive suggestions. Jie Cai participated in the experiment. Zhirui Li and Minjie Li performed the data proofreading. All authors revised the report and approved the final version before submission.

Data availability The data will be available on request.

Ethics approval and consent to participate Not applicable

Consent for publication Not applicable

Competing interests The authors declare no competing interests

6. References

1. Adjaye JD, Bakhshi NN (1995) Catalytic conversion of a biomass-derived oil to fuels and chemicals I: Model compound studies and reaction pathways. Biomass Bioenerg 8:131–149. https://doi.org/10.1016/0961-9534(95)00018-3
2. Aguado J, Serrano DP, Sotelo JL et al (2001) Influence of the Operating Variables on the Catalytic Conversion of a Polyolefin Mixture over HMCM-41 and Nanosized HZSM-5. Ind Eng Chem Res 40:5696–5704. https://doi.org/10.1021/ie010420c
3. Ahmed II, Nipattummakul N, Gupta AK (2011a) Characteristics of syngas from co-gasification of polyethylene and woodchips. Appl Energy 88:165–174. https://doi.org/10.1016/j.apenergy.2010.07.007
4. Ahmed II, Nipattummakul N, Gupta AK (2011b) Characteristics of syngas from co-gasification of polyethylene and woodchips. Appl Energy 88:165–174. https://doi.org/10.1016/j.apenergy.2010.07.007
5. Areeprasert C, Asingsamanunt J, Srisawat S et al (2017) Municipal Plastic Waste Composition Study at Transfer Station of Bangkok and Possibility of its Energy Recovery by Pyrolysis. Energy Procedia 107:222–226. https://doi.org/10.1016/j.egypro.2016.12.132
6. Barbarias I, Lopez G, Amutio M et al (2016a) Steam reforming of plastic pyrolysis model hydrocarbons and catalyst deactivation. Appl Catal A 527:152–160. https://doi.org/10.1016/j.apcata.2016.09.003
7. Barbarias I, Lopez G, Amutio M et al (2016b) Steam reforming of plastic pyrolysis model hydrocarbons and catalyst deactivation. Appl Catal A 527:152–160. https://doi.org/10.1016/j.apcata.2016.09.003

8. Bhattacharya P, Steele PH, Hassan EBM et al (2009) Wood/plastic copyrolysis in an auger reactor: Chemical and physical analysis of the products. Fuel 88:1251–1260. https://doi.org/10.1016/j.fuel.2009.01.009
9. Carpenter DL, Bain RL, Davis RE et al (2010) Pilot-Scale Gasification of Corn Stover, Switchgrass, Wheat Straw, and Wood: 1. Parametric Study and Comparison with Literature. Ind Eng Chem Res 49:1859–1871. https://doi.org/10.1021/ie900595m
10. Dong C, Yang Y, Jin B, Horio M (2007) The pyrolysis of sawdust and polyethylene in TG and U-shape tube reactor. Waste Manag 27:1557–1561. https://doi.org/10.1016/j.wasman.2006.10.021
11. Fagbemi L (2002) Pyrolysis products from different biomasses: application to the thermal cracking of tar. Fuel Energy Abstracts 43:279. https://doi.org/10.1016/S0140-6701(02)86434-7
12. Gayubo AG, Aguayo AT, Atutxa A et al (2004) Transformation of Oxygenate Components of Biomass Pyrolysis Oil on a HZSM-5 Zeolite. I. Alcohols and Phenols. Ind Eng Chem Res 43:2610–2618. https://doi.org/10.1021/ie030791o
13. Giovanna Ruoppolo F, Miccio P, Brachi et al (2013) Fluidized bed gasification of biomass and biomass/coal pellets in oxygen and steam atmosphere. Chem Eng Trans 32:595–600. https://doi.org/10.3303/CET1332100
14. Göransson K, Söderlind U, Zhang W (2011) Experimental test on a novel dual fluidised bed biomass gasifier for synthetic fuel production. Fuel 90:1340–1349. https://doi.org/10.1016/j.fuel.2010.12.035
15. Hájeková E, Bajus M (2005) Recycling of low-density polyethylene and polypropylene via copyrolysis of polyalkene oil/waxes with naphtha: product distribution and coke formation. J Anal Appl Pyrol 74:270–281. https://doi.org/10.1016/j.jaap.2004.11.016
16. Hu B, Huang Q, Buekens A et al (2017) Co-gasification of municipal solid waste with high alkali coal char in a three-stage gasifier. Energy Convers Manag 153:473–481. https://doi.org/10.1016/j.enconman.2017.10.026
17. Li X, Li J, Zhou G et al (2014) Enhancing the production of renewable petrochemicals by co-feeding of biomass with plastics in catalytic fast pyrolysis with ZSM-5 zeolites. Appl Catal A 481:173–182. https://doi.org/10.1016/j.apcata.2014.05.015
18. Li XT, Grace JR, Lim CJ et al (2004) Biomass gasification in a circulating fluidized bed. Biomass Bioenerg 26:171–193. https://doi.org/10.1016/S0961-9534(03)00084-9
19. Long Y, Li Q, Zhou H et al (2017) Pseudo-component method for characterization of the thermochemical conversion of combustible solid waste. Journal of Tsinghua University(Science Technology) 57:1324–1330. https://doi.org/10.16511/j.cnki.qhdxxb.2017.25.056
20. Lopez G, Erkiaga A, Amutio M et al (2015) Effect of polyethylene co-feeding in the steam gasification of biomass in a conical spouted bed reactor. Fuel 153:393–401. https://doi.org/10.1016/j.fuel.2015.03.006
21. Lu P, Huang Q, Chi Y et al (2019) Catalytic cracking of tar derived from the pyrolysis of municipal solid waste fractions over biochar. Proceedings of the Combustion Institute 37:2673–2680. https://doi.org/10.1016/j.proci.2018.06.051

22. Lu P, Huang Q, (Thanos) Bourtsalas AC et al (2018) Synergistic effects on char and oil produced by the co-pyrolysis of pine wood, polyethylene and polyvinyl chloride. Fuel 230:359–367. https://doi.org/10.1016/j.fuel.2018.05.072
23. Lukyanov D, Gnep N, Guisnet M (1994) Kinetic modeling of ethene and propene aromatization over HZSM-5 and GaHZSM-5. Industrial Engineering Chemistry Research - IND ENG CHEM RES 33:223–234. https://doi.org/10.1021/ie00026a008
24. Marcilla A, Beltrán MI, Navarro R (2006) TG/FT-IR analysis of HZSM5 and HUSY deactivation during the catalytic pyrolysis of polyethylene. J Anal Appl Pyrol 76:222–229. https://doi.org/10.1016/j.jaap.2005.11.008
25. Montero C, Ochoa A, Castaño P et al (2015) Monitoring Ni 0 and coke evolution during the deactivation of a Ni/La 2 O 3 –αAl 2 O 3 catalyst in ethanol steam reforming in a fluidized bed. J Catal 331:181–192. https://doi.org/10.1016/j.jcat.2015.08.005
26. Pinto F, André R, Miranda M et al (2016) Effect of gasification agent on co-gasification of rice production wastes mixtures. 10
27. Pinto F, André RN, Lopes H et al (2012) Comparison of a pilot scale gasification installation performance when air or oxygen is used as gasification medium 2 – Sulphur and nitrogen compounds abatement. Fuel 97:770–782. https://doi.org/10.1016/j.fuel.2012.02.031
28. Pinto F, Franco C, André RN et al (2002) Co-gasification study of biomass mixed with plastic wastes. Fuel 81:291–297. https://doi.org/10.1016/S0016-2361(01)00164-8
29. Rama S, Kawai S, Yamada H, Tagawa T (2014) Preliminary Assessment of Oxidation Pretreated Hastelloy as Hydrocarbon Steam Reforming Catalyst. Journal of Catalysts 2014:1–7. https://doi.org/10.1155/2014/210371
30. Shurong W (2017) Lignocellulosic biomass pyrolysis mechanism: A state-of-the-art review. Progress in Energy and Combustion Science 54
31. Sørum L, Grønli MG, Hustad JE (2001) Pyrolysis characteristics and kinetics of municipal solid wastes. Fuel 80:1217–1227. https://doi.org/10.1016/S0016-2361(00)00218-0
32. Tang Y, Huang Q, Sun K et al (2018) Co-pyrolysis characteristics and kinetic analysis of organic food waste and plastic. Biores Technol 249:16–23. https://doi.org/10.1016/j.biortech.2017.09.210
33. Tursun Y, Xu S, Wang C et al (2016) Steam co-gasification of biomass and coal in decoupled reactors. Fuel Processing Technology 141:61–67. https://doi.org/10.1016/j.fuproc.2015.06.046
34. Vicente J, Montero C, Ereña J et al (2014) Coke deactivation of Ni and Co catalysts in ethanol steam reforming at mild temperatures in a fluidized bed reactor. Int J Hydrogen Energy 39:12586–12596. https://doi.org/10.1016/j.ijhydene.2014.06.093
35. Wampler TP (1989) Thermometric behavior of polyolefins. J Anal Appl Pyrol 15:187–195. https://doi.org/10.1016/0165-2370(89)85032-6
36. Wen J, Chi Y, Jin Y et al (2005) Experimental study on msw pyrolysis and its neural networks prediction model. Proceedings of the CSEE 156–160
37. Wen J, Chi Y, Luo C et al (2004) Study on the pyrolysis characteristics of the mixture of typical organic components of MSW. Journal of Fuel Chemistry and Technology 563–568

38. Wilk V, Hofbauer H (2013) Co-gasification of Plastics and Biomass in a Dual Fluidized-Bed Steam Gasifier: Possible Interactions of Fuels. Energy Fuels 27:3261–3273. https://doi.org/10.1021/ef400349k
39. Zheng X, Chen C, Ying Z, Wang B (2016) Experimental study on gasification performance of bamboo and PE from municipal solid waste in a bench-scale fixed bed reactor. Energy Convers Manag 117:393–399. https://doi.org/10.1016/j.enconman.2016.03.044

Figures

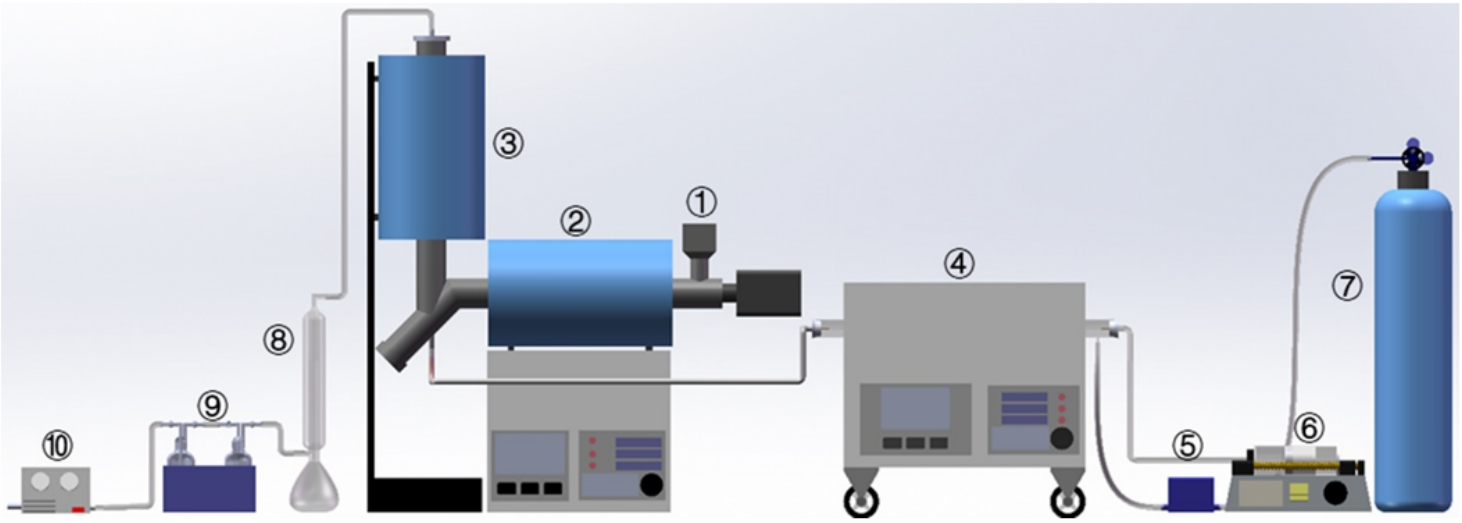

Figure 1

Schematic representation of the laboratory scale apparatus. (Screw feeder Tubular furnace(first) Tubular furnace (second) Steam generator Electronic flowmeter Injection pump nitrogen cylinder Condenser Tar trap Vacuum pump)

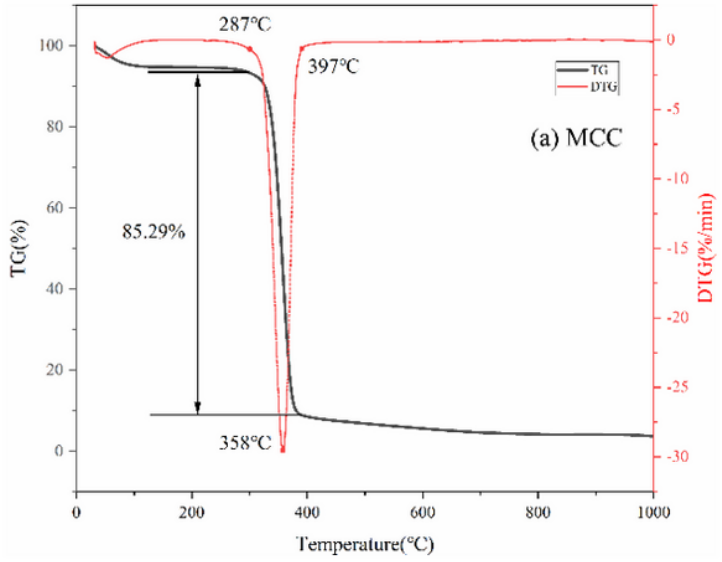

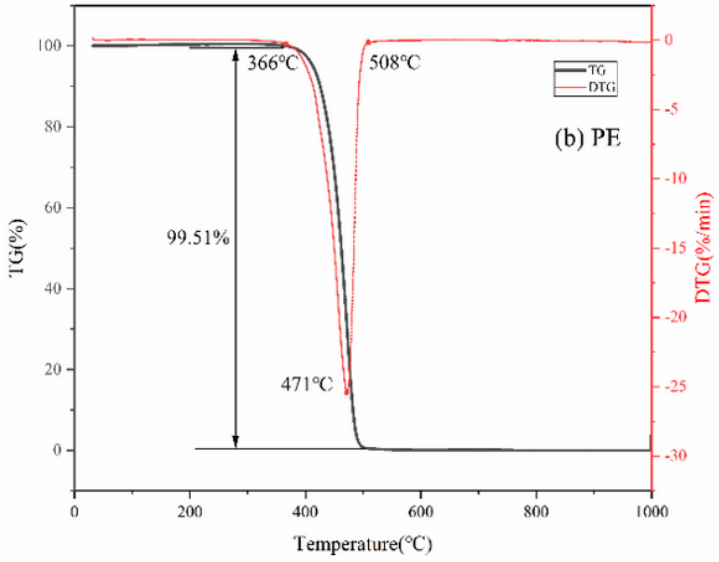

Figure 2

TG and DTG of (a) MCC, (b) PE.

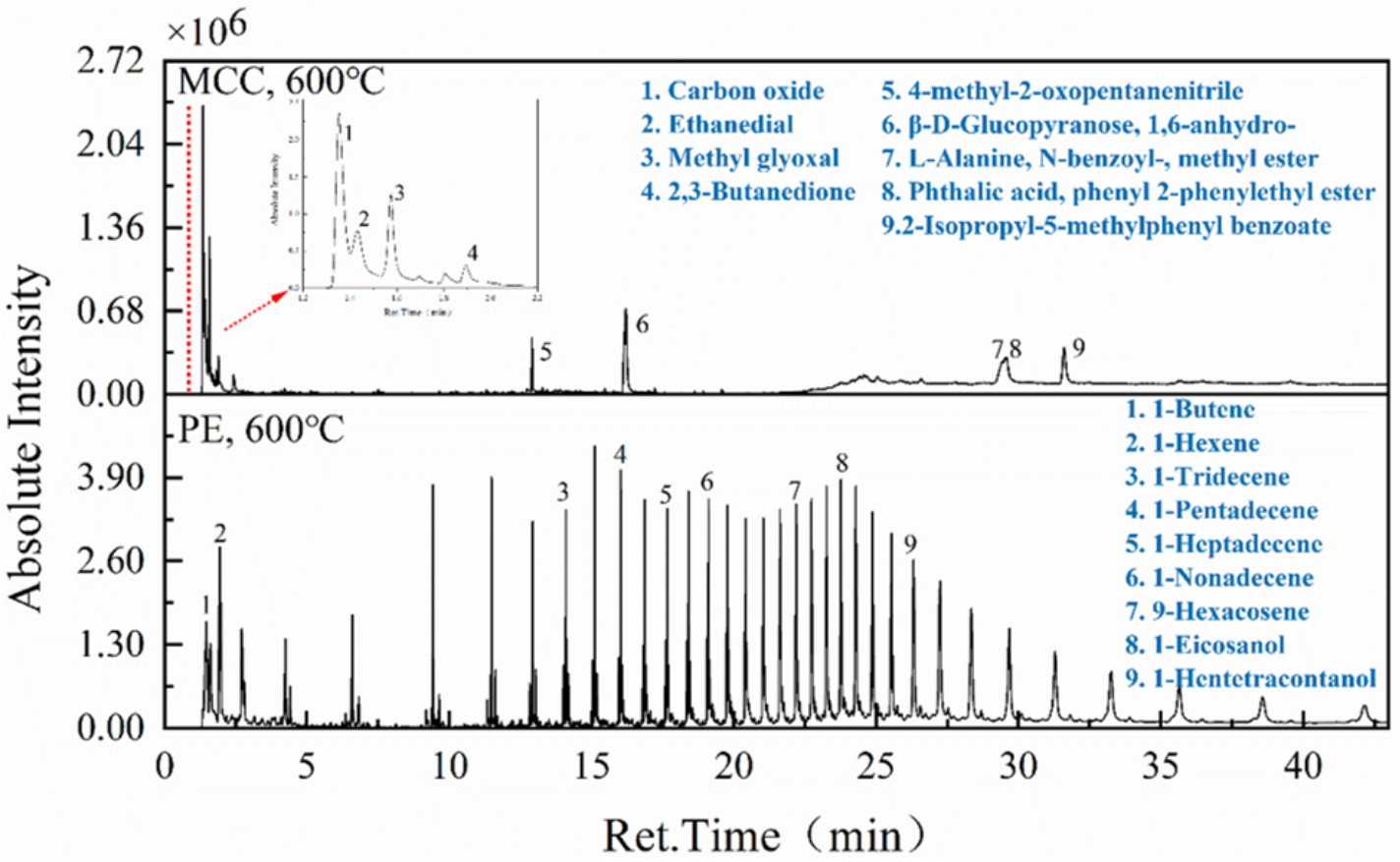

Figure 3

Chromatograms of products in fast pyrolysis of (a) MCC, (b) PE at 600°C.

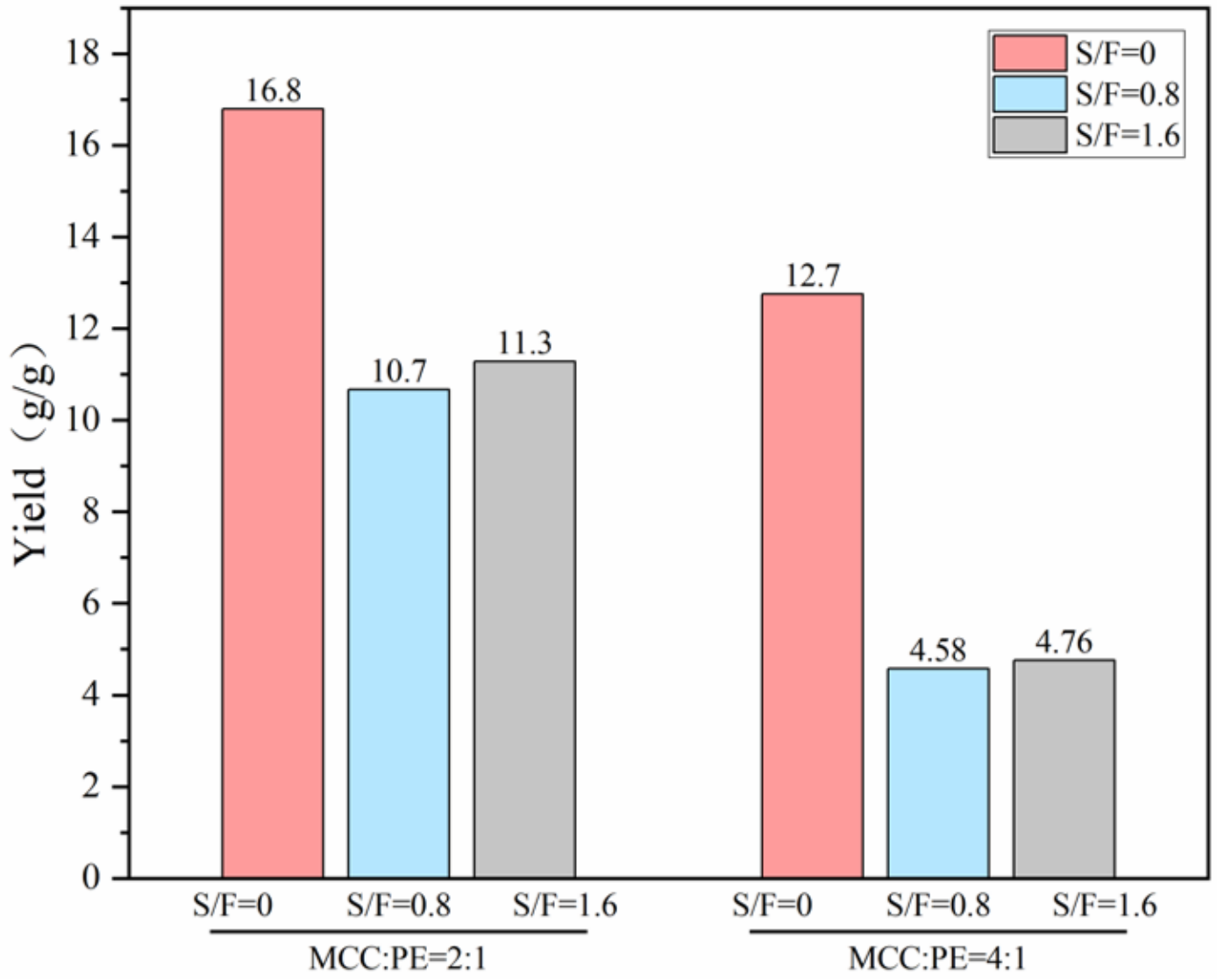

Figure 4

The yield of tar produced from co-feeding experiments in a two-stage apparatus (the first stage was 600℃, and the second stage was 800 ℃).

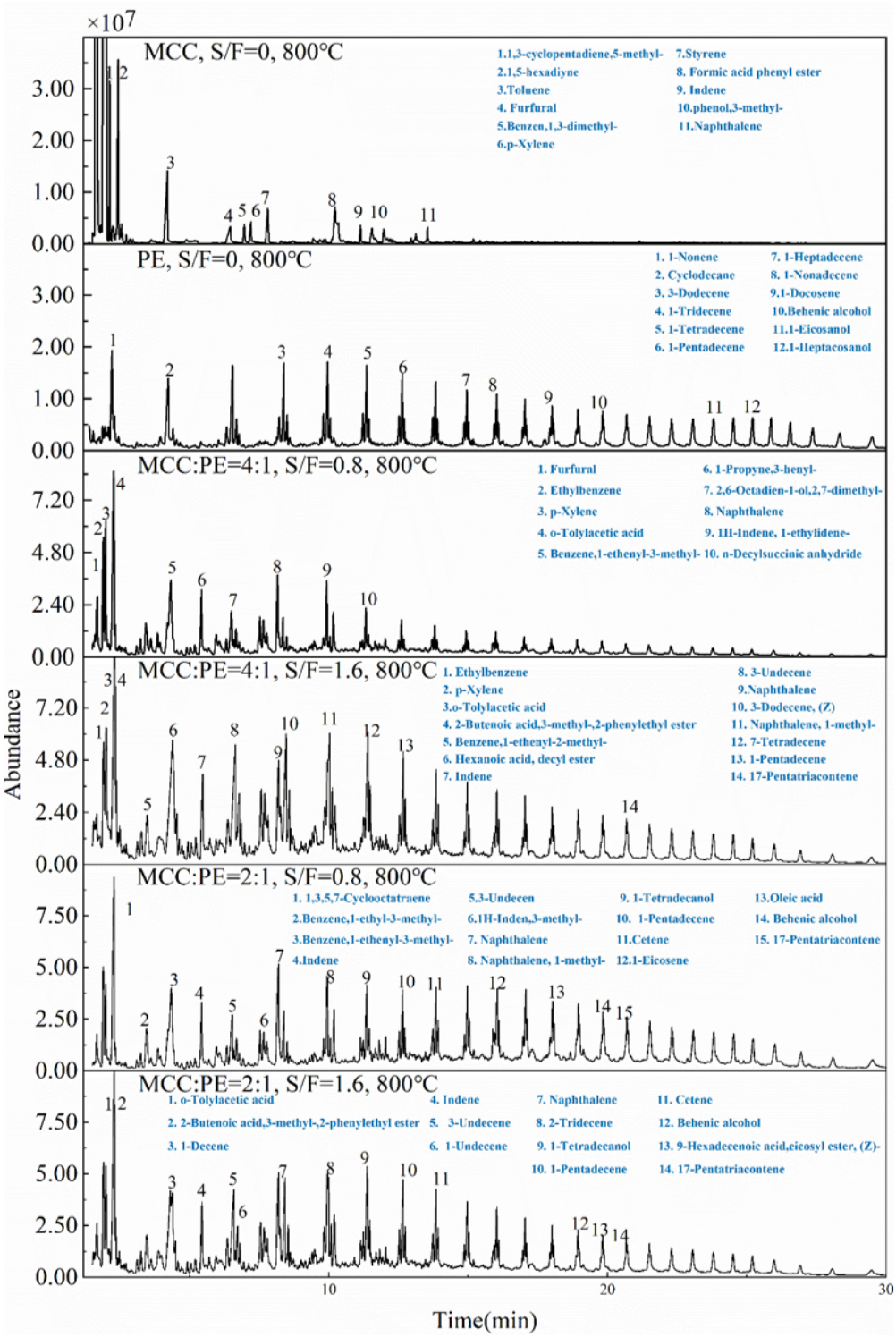

Figure 5

Chromatograms of tar produced from co-feeding experiments.

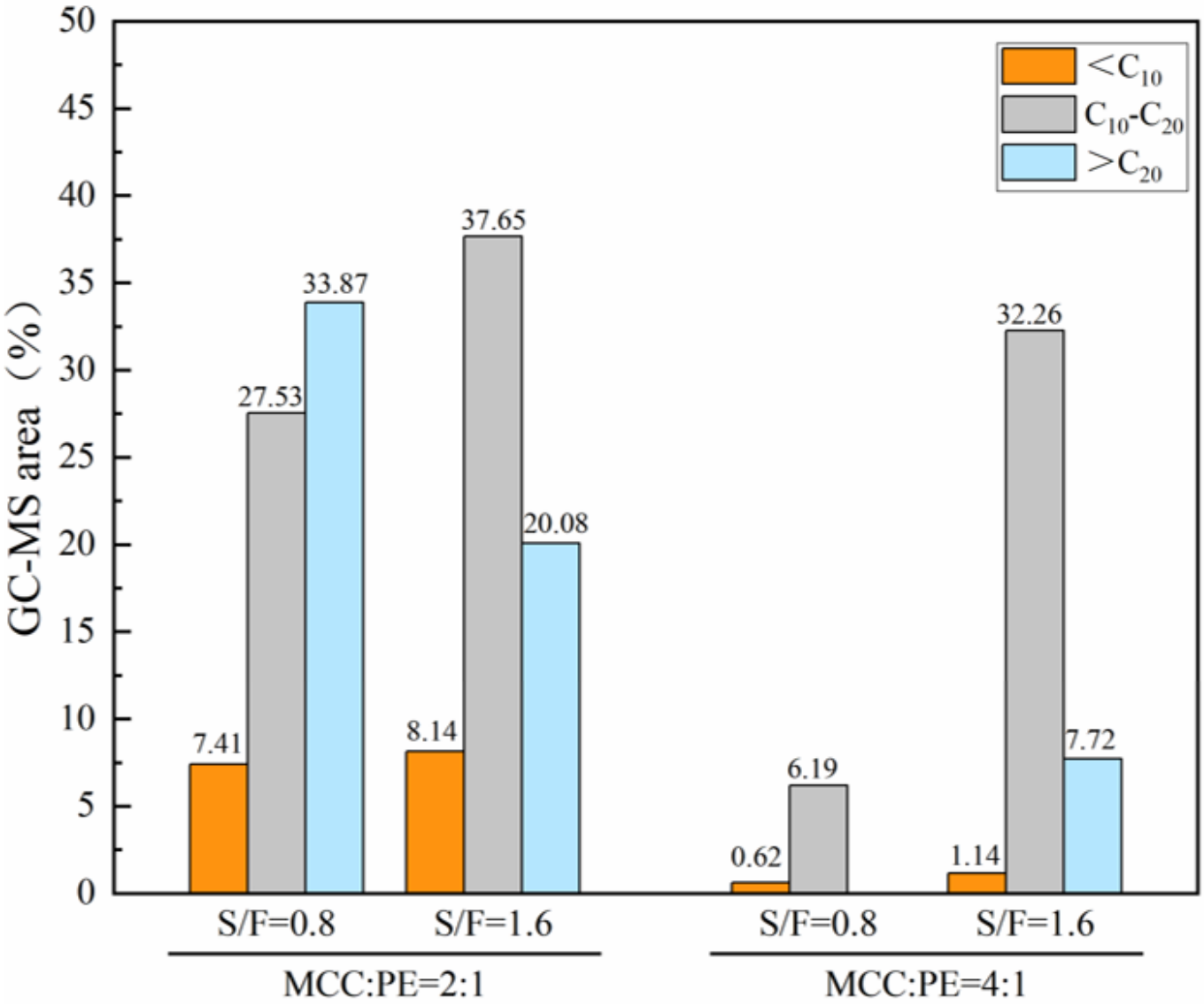

Figure 6

The distribution of chain hydrocarbons and their derivatives.

Supplementary Files

This is a list of supplementary files associated with this preprint. Click to download.

- GraphicalAbstract.png
- AppendixA.docx